Preprints.org

Article

Not peer-reviewed version

The Mechanistic Evaluation of Danggui Buxue Tang, an Ancient Chinese Herbal Decoction Containing Astragali Radix and Angelicae Sinensis Radix, by Network Pharmacology

Ghodsiehsadat Jahanmir , Shengying Lin , Ajiaikebaier Dilidaer , Jin Gao , Ka Wing Leung , Karl Wah Keung Tsim *

Posted Date: 5 September 2025

doi: 10.20944/preprints202509.0511.v1

Keywords: Danggui Buxue Tang; traditional Chinese medicine; network pharmacology; target–pathway network

Preprints.org is a free multidisciplinary platform providing preprint service that is dedicated to making early versions of research outputs permanently available and citable. Preprints posted at Preprints.org appear in Web of Science, Crossref, Google Scholar, Scilit, Europe PMC.

Copyright: This open access article is published under a Creative Commons CC BY 4.0 license, which permit the free download, distribution, and reuse, provided that the author and preprint are cited in any reuse.

Preprints.org (www.preprints.org) | NOT PEER-REVIEWED | Posted: 5 September 2025 doi:10.20944/preprints202509.0511.v1

Disclaimer/Publisher's Note: The statements, opinions, and data contained in all publications are solely those of the individual author(s) and contributor(s) and not of MDPI and/or the editor(s). MDPI and/or the editor(s) disclaim responsibility for any injury to people or property resulting from any ideas, methods, instructions, or products referred to in the content.

Article

The Mechanistic Evaluation of Danggui Buxue Tang, an Ancient Chinese Herbal Decoction Containing Astragali Radix and Angelicae Sinensis Radix, by Network Pharmacology

Ghodsiehsadat Jahanmir [1,2], Shengying Lin [1,2], Ajiaikebaier Dilidaer [1], Jin Gao [1,3], Ka Wing Leung [1,2] and Karl Wah Keung Tsim [1,2,*]

[1] Division of Life Science, Center for Chinese Medicine and State Key Laboratory of Molecular Neuroscience, The Hong Kong University of Science and Technology, Hong Kong, China

[2] Shenzhen Key Laboratory of Edible and Medicinal Bioresources, The Hong Kong University of Science and Technology, Shenzhen, China

[3] Department of Neurobiology and Cellular Biology, Xuzhou Medical University, Xuzhou, Jiangsu, China

* Correspondence: botsim@eust.hk

Abstract

Background/Objectives: Danggui Buxue Tang (DBT), an herbal formula deriving from traditional Chinese medicine (TCM), is widely recognized for its therapeutic effectiveness in clinical practice. To uncover the molecular mechanisms underlying its therapeutic actions and identify potential therapeutic targets, we employ a novel network pharmacology approach. **Methods:** Active compounds were retrieved from the TCMSP database, and their corresponding protein targets were identified using existing databases, such as TCMSP, ETCM v2.0, Herb v2.0, and Swiss Target Prediction. These target genes were then functionally annotated via STRING, focusing on Gene Ontology categories (Biological Process, Cellular Component, and Molecular Function), KEGG pathways, and disease associations. A "targets–(pathways)–targets" network was constructed to connect DBT's targets through the shared signaling pathways. The network was further divided into distinct modules with strong internal connectivity. Using a contribution scoring algorithm, the association of each module with various diseases was evaluated, highlighting those with significant relevance. **Results:** The key targets with the module having the highest relevance to common diseases within the DBT's categories were proposed as promising therapeutic candidates**. Conclusions:** By integrating complex interactions among targets, pathways, and diseases, this approach provides a robust framework in elucidating the mechanisms of action of a herbal mixture and supports the scientific validation of its traditional uses.

Keywords: Danggui Buxue Tang; traditional Chinese medicine; network pharmacology; target–pathway network

1. Introduction

Danggui Buxue Tang (DBT) is an ancient Chinese herbal decoction, which consists of Astragali Radix (AR; roots of *Astragalus membranaceus* (Fisch). Bunge or *A. membranaceus* (Fisch). Bunge var. *mongholicus* (Bunge) Hsiao) and Angelicae Sinensis Radix (ASR; roots of *Angelica sinensis* Oliv) at the weight ratio of 5:1 [1–4] recorded in "Neiwaishang Bianhuo Lun" by Li Dongyuan in Jin dynasty (about AD 1247). Traditionally, DBT is used to tonify "qi" (vital energy) and nourish "blood". In clinical practice, it is well known to treat women's blood-deficiency conditions, such as menopausal or post-partum weakness [2]. DBT exerts multi-faceted pharmacological actions consistent with its traditional usages. DBT has been shown to stimulate hematopoiesis and modulate immune function

© 2025 by the author(s). Distributed under a Creative Commons CC BY license.

Preprints.org (www.preprints.org) | NOT PEER-REVIEWED | Posted: 5 September 2025 doi:10.20944/preprints202509.0511.v1

[3,4], in line with its claims of "blood-enriching", which also displays systemic protective effects, including estrogenic activity, bone regeneration, cardiovascular and pulmonary protection, and promotion of capillary (blood vessel) formation. *In vitro* assays demonstrate antioxidative and bioenergetic benefits of DBT in different cell types [1,5–7]. Besides, DBT reduced inflammatory reaction in mouse models, e.g., restoring the colonic tissue of dextran sulfate sodium-induced inflammatory bowel disease, as well as repairing intestinal epithelial cells [8].

Network pharmacology and molecular docking approaches have been used to dissect the complex mechanism of DBT. The analyses highlighted the signaling pathways, such as PI3K–Akt, as well as the experimental validation in the DBT-induced hematopoiesis to nourish blood [9]. In addition, integrative approaches to elucidate the DBT mechanism have been employed in treating anemia in rats using serum metabolomics, network pharmacology and molecular docking [10,11]. Similar approach has been applied in studying the roles of DBT in lung cancer [12,13], ulcerative colitis [14], atherosclerosis [15,16], myocardial infarction [17] and in vascular dementia rats [18].

Although the aforementioned results are informative, these studies are anchored to specific pathological models, instead of capturing the full multi-target profile of DBT functions. Here, we aim to provide disease-agnostic network models of DBT. The phytochemicals within DBT were probed for ADME properties, and their putative/validated targets were postulated from various databases, e.g., TSMSP, ETCM v2.0, and HERB v2.0. The GO terms and relevant pathways were extracted using the STRING database, as to establish the target-pathway interactions.

The diseases linked to these pathways were developed, and which generated the "targets-(pathways)-targets" (TPT) network in which the nodes representing the targets. The edges between nodes represent the shared pathways among the targeted genes. An algorithm was utilized to detect communities among the nodes of the network, as to assess the contribution of each module to different diseases, The contribution scores were compared among target communities, and the top targets from the modules with the highest scores relating to relevant DBT-treated diseases were identified.

2. Results

2.1. Bioactive Compounds and Target Predictions

The DBT decoction consists of two herbal constituents: Astragali Radix and Angelicae Sinensis Radix. Initial phytochemical profiling using TCMSP identified 87 compounds in Astragali Radix and 125 in Angelicae Sinensis Radix. Pharmacokinetic filtering (OB >30%, DL >0.18) resulted in 20 candidates having considered bioactive molecules, with 18 derived from Astragali Radix and 2 from Angelicae Sinensis Radix. **Table 1** summarizes these compounds; their PubChem identification numbers and pharmacokinetic parameters.

Table 1. Filtered compounds of DBT and their properties obtained from the TCMSP database, including their PubChem Compound Identification Number (PubChem CID).

PubChem CID	Compound name	OB[a] (%)	DL[b]
64971	Mairin	55.38	0.78
5318869	Jaranol	50.83	0.29
73299	Hederagenin	36.91	0.75
15976101	(3S,8S,9S,10R,13R,14S,17R)-10,13-dimethyl-17-[(2R,5S)-5-propan-2-yloctan-2-yl]-2,3,4,7,8,9,11,12,14,15,16,17-dodecahydro-1H-cyclopenta[a]phenanthren-3-ol	36.23	0.78
5281654	Isorhamnetin	49.6	0.31
15689655	3,9-di-O-methylnissolin	53.74	0.48
Not Found	5'-hydroxyiso-muronulatol-2',5'-di-O-glucoside	41.72	0.69
15689652	7-O-methylisomucronulatol	74.69	0.3
86566448	9,10-dimethoxypterocarpan-3-O-β-D-glucoside	36.74	0.92

© 2025 by the author(s). Distributed under a Creative Commons CC BY license.

Preprints.org (www.preprints.org) | NOT PEER-REVIEWED | Posted: 5 September 2025 doi:10.20944/preprints202509.0511.v1

14077830	(6aR,11aR)-9,10-dimethoxy-6a,11a-dihydro-6H-benzofurano[3,2-c]chromen-3-ol	64.26	0.42
108213	Bifendate	31.1	0.67
5280378	Formononetin	69.67	0.21
160767	Isoflavanone	109.99	0.3
5280448	Calycosin	47.75	0.24
5280863	Kaempferol	41.88	0.24
6037	FA	68.96	0.71
10380176	(3R)-3-(2-hydroxy-3,4-dimethoxyphenyl)chroman-7-ol	67.67	0.26
15689653	Isomucronulatol-7,2'-di-O-glucosiole	49.28	0.62
5316760	1,7-Dihydroxy-3,9-dimethoxypterocarpene	39.05	0.48
5280343	Quercetin	46.43	0.28
222284	Beta-sitosterol	36.91	0.75
5280794	Stigmasterol	43.83	0.76

[a]OB: Oral Bioavailability; [b]DL: Drug-Likeness.

Compound-protein interactions were systematically retrieved by interrogating four pharmacological repositories: TCMSP, ETCM v2.0, Herb v2.0, and Swiss Target Prediction. The targets from TCMSP lacked gene symbols, so that the nomenclature standardization was achieved through cross-referencing with Uniprot database to resolve gene symbols and primary accession identifiers. After de-duplication and the removal of non-human listed genes, a consolidated dataset comprising 651 unique human protein targets was generated for subsequent network pharmacology analyses. **Table S1** presents a comprehensive list of compounds along with their corresponding targets and database reference.

2.2. GO and KEGG Pathway Enrichment

Analysis of the 651 DBT-associated targets using STRING database revealed 3,406 statistically significant Gene Ontology (GO) terms (FDR <0.05), which included 2,891 biological processes (BP), 174 cellular components (CC), and 341 molecular functions (MF). **Figure 1** presents the top 10 most significantly enriched terms (p <0.05) in each GO category, visualized using bar plots. The key biological processes primarily involved cellular and systemic responses to oxygen-containing compounds, xenobiotic stimuli, organic substances, and endogenous biochemical signals. The analysis of cellular components indicated a predominant localization in cytoplasmic and vesicular compartments, particularly in the cytosol, plasma membrane regions, extracellular space, and organelle lumens. The molecular functions were largely characterized by protein-protein interaction modalities (enzyme binding, identical protein binding, signaling receptor binding, kinase binding) and catalytic activities, with additional enrichment in ion binding (transition metal ions).

© 2025 by the author(s). Distributed under a Creative Commons CC BY license.

Preprints.org (www.preprints.org) | NOT PEER-REVIEWED | Posted: 5 September 2025 doi:10.20944/preprints202509.0511.v1

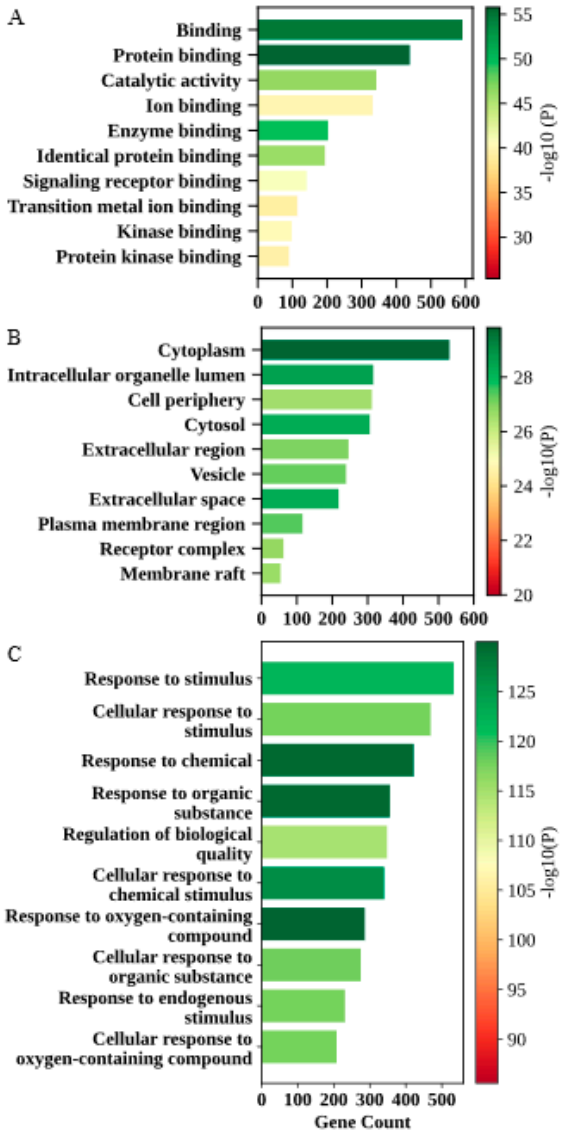

Figure 1. Enrichment of the top 10 Gene Ontology (GO) terms of DBT.The top 10 identified GO in (A) Molecular Function, (B) Cellular Component, and (C) Biological Process categories for the gene targets of DBT. GO term enrichment was performed using the STRING database (version 12.0; accessed Aug 2025), with terms ranked by the number of associated genes (x-axis). Bar colors represent the strength of enrichment, shown as $-\log_{10}$ (*P*-value), with a false discovery rate (FDR) threshold of 0.05.

A total of 227 significant pathways associated with 552 relevant protein targets of DBT were enriched, as derived from STRING database. The top 20 enriched pathways, visualized as bar plots in Figure 2, indicated strong involvement in human disease pathways, including cancer pathways, Alzheimer's disease, human cytomegalovirus infection, fluid shear stress and atherosclerosis, AGE-RAGE signaling pathway in diabetic complications, and hepatitis B. Additionally, the pathways related to environmental information processing, such as neuroactive ligand-receptor interaction, PI3K-Akt signaling pathway, and MAPK signaling pathway, were highlighted along with cellular processes like cellular senescence (Figure 3, classification of pathways based on KEGG mapping).

© 2025 by the author(s). Distributed under a Creative Commons CC BY license.

Preprints.org (www.preprints.org) | NOT PEER-REVIEWED | Posted: 5 September 2025 doi:10.20944/preprints202509.0511.v1

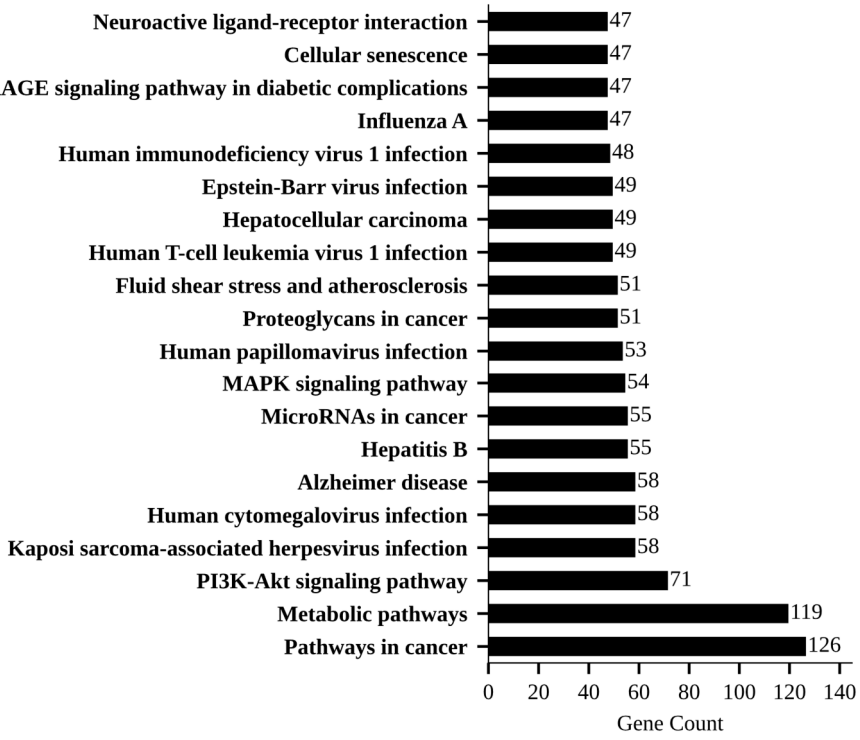

Figure 2. Enrichment of the top 20 KEGG pathways of DBT-targeted genes.The identification was via STRING database (version 12.0; accessed Aug 2025). Pathway enrichment analysis (false discovery rate < 0.05) yielded pathways (shown top 20) sorted by the number of DBT targets mapped to each (x-axis). The most enriched pathways include "Pathways in cancer (hsa05200)," "Metabolic pathways(hsa01100)" , "PI3K–Akt signaling pathway(hsa04151)", "Kaposi sarcoma-associated herpesvirus infection(hsa05167)", "Human cytomegalovirus infection(hsa05163)", "Alzheimer's disease (hsa05010)", "Hepatitis B (hsa05161)", "MicroRNAs in cancer (hsa05206)", and "MAPK signaling pathway (hsa04010)", underscoring DBT's potential roles in oncogenesis, metabolism, viral responses, neurodegeneration, and cell signaling.

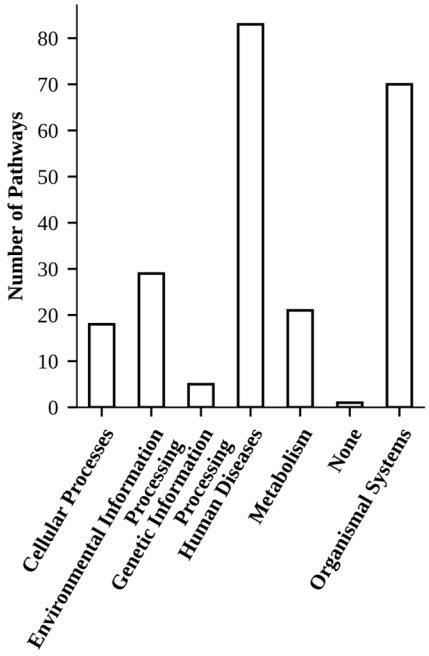

© 2025 by the author(s). Distributed under a Creative Commons CC BY license.

Preprints.org (www.preprints.org) | NOT PEER-REVIEWED | Posted: 5 September 2025 doi:10.20944/preprints202509.0511.v1

Figure 3. Classification of 227 significantly enriched KEGG pathways of DBT. The pathways were mapped to six top-level KEGG pathway classes—Metabolism; Genetic Information Processing; Environmental Information Processing; Cellular Processes; Organismal Systems; and Human Diseases—using the KEGG pathway hierarchy (https://www.kegg.jp/kegg/pathway.html). Enrichment was determined by KEGG pathway enrichment analysis (false discovery rate < 0.05). The bar chart indicates that Human disease accounts for the largest share of enriched pathways (n = 83), followed by Organismal systems (n = 70) highlighting the broad modulatory effects of DBT across core biological functions.

Pathway-disease mapping analysis (KEGG Pathways → KEGG Gene → KEGG Disease) of the 227 KEGG pathways identified 30 major disease categories with potential therapeutic associations. The predominant disease classifications included nervous system diseases, congenital malformations, inherited metabolic disorders, cancer, immune system diseases, cardiovascular diseases, hematologic diseases, mitochondrial disorders, and peroxisomal diseases (Table S2).

2.3. Community Detection in Target-Pathway-Target Network

Utilizing the 552 targets mapping to 227 relevant pathways, we constructed a target-pathway-target (TPT) network comprising 552 nodes and 35,218 edges. In this network, each node represents a distinct target, while the edges indicate that the connected nodes are co-enriched in at least one specific pathway. To identify target communities within the TPT network, we employed Louvain algorithm, implemented through the CyCommunity Detection App in Cytoscape 3.10.3, with a cluster resolution parameter set to 1.0. Ultimately, four target modules were identified and categorized. Detailed target protein distribution regarding these four target modules is provided in **Table S3**.

The most prevalent pathways within modules 1 to 4 are metabolic pathways (hsa01100), NOD-like receptor signaling pathway (hsa04621), pathways in cancer (hsa05200), and neuroactive ligand–receptor interaction (hsa04080), as summarized in **Table 2**. Module 1 is primarily characterized by metabolic pathways, while modules 2 and 3 are associated with human disease pathways. Module 4 exhibits a higher frequency of environmental information processing pathways. Modules 2 and 3 also demonstrate greater diversity in their pathway associations. A detailed list of pathway frequencies across modules is provided in **Table S4**.

Table 2. Protein module enrichment profiles for four non-overlapping protein modules.

Module[a]	**1**	**2**	**3**	**4**
Top Frequent Pathway identifier	hsa01100	hsa04621	hsa05200	hsa04080
Pathway name	Metabolic pathways	NOD-like receptor signaling pathway	Pathways in cancer	Neuroactive ligand-receptor interaction
Repeated times	6555	703	3403	1081
Total pathways in module	8328	16064	25471	3732
Number of unique pathways in module	86	145	178	106

[a]The listing for each the top KEGG pathway (ID and name), its recurrence ("Repeated times"), the total pathway assignments in the module ("Total pathways in module"), and the number of distinct pathways detected ("Number of unique pathways in module").

2.4. Disease Association Analysis

Building on the observations from the previous section, it appears that the target modules within the TPT network may represent distinct biological functions. Having the identification of the four key

© 2025 by the author(s). Distributed under a Creative Commons CC BY license.

Preprints.org (www.preprints.org) | NOT PEER-REVIEWED | Posted: 5 September 2025 doi:10.20944/preprints202509.0511.v1

modules, we applied a contribution scoring algorithm to assess their relevance across 30 different diseases. The results, as presented as a heatmap in **Figure 4**, display modules as columns and diseases as rows, with the intensity of each cell reflecting the strength of association between a given module and a disease.

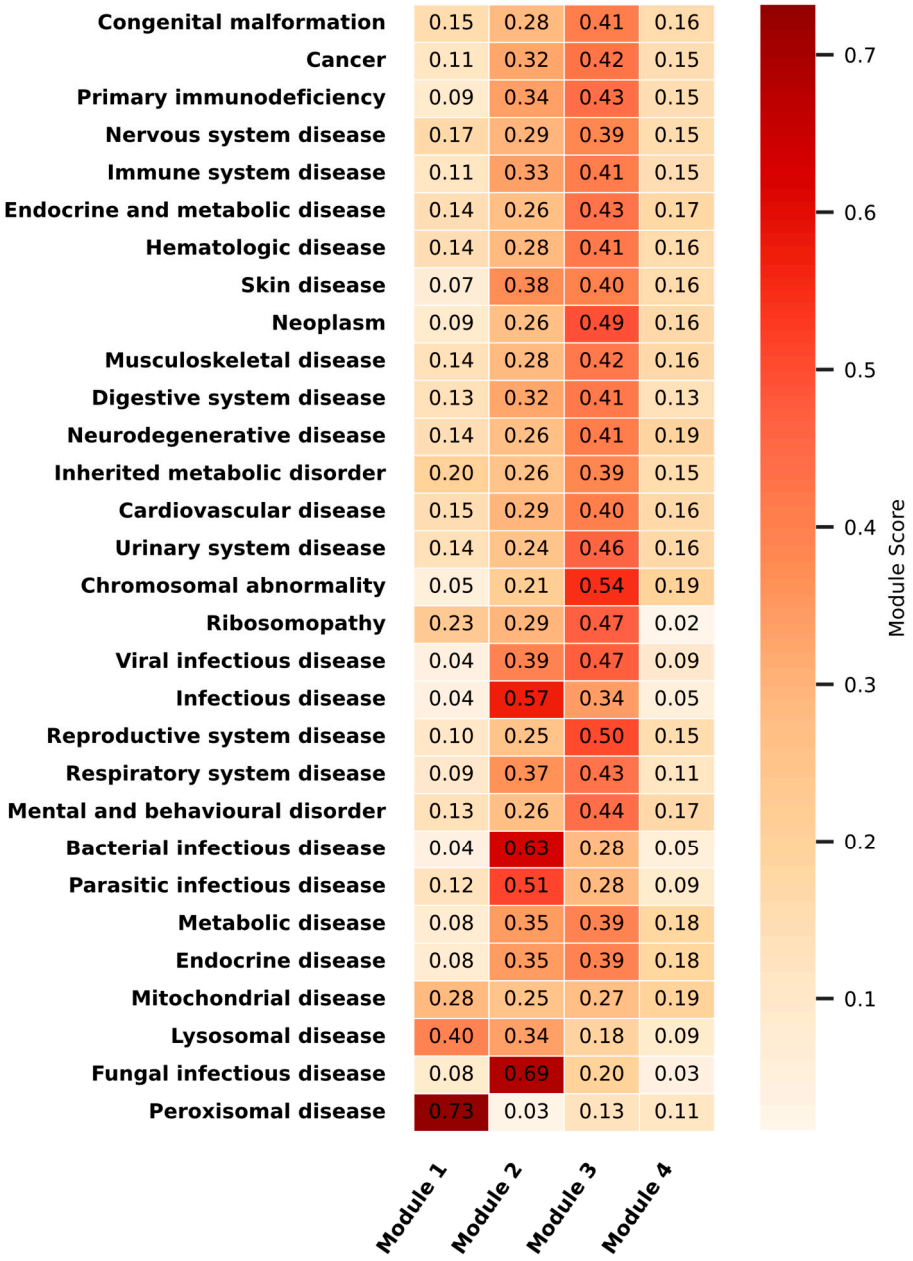

Figure 4. Heatmap shows the contribution scores of four gene-target modules of DBT across various disease categories. For each gene–disease category pair, a contribution score was calculated based on pathway–gene–disease associations. These scores were then aggregated within each module and expressed as the proportion of module genes associated with pathways linked to a given disease category. Scores range from 0 (white) to 1 (deep red), with darker shades indicating a stronger contribution of the module to that disease category.

The analysis reveals clear and unique patterns among the modules. For instance, module 1 shows a strong association with peroxisomal disease, while module 2 is more closely linked to infectious diseases. Module 3 exhibits broader relevance, contributing significantly to multiple disease categories, including cancer, nervous system disorders, immune-related conditions, endocrine and metabolic diseases, as well as hematologic, reproductive, and neurodegenerative

© 2025 by the author(s). Distributed under a Creative Commons CC BY license.

Preprints.org (www.preprints.org) | NOT PEER-REVIEWED | Posted: 5 September 2025 doi:10.20944/preprints202509.0511.v1

disorders. These distinct profiles suggest that each module may play a specific therapeutic role within the TPT network, likely reflecting different functional mechanisms. Overall, the findings reinforce the idea that the active components of DBT may exert their effects through diverse pathways, targeting various diseases—a notion supported by prior studies [19,20].

In the subsequent analysis, we pinpointed the target module with the highest relevance to DBT-related diseases, as outlined in **Table 3**. Although not comprehensive, **Table 3** categorizes the general disease areas where DBT is applied. Among the seven disease categories listed here, module 3 emerged with the highest score, as depicted in **Figure 4**, indicating potential therapeutic effects of DBT on the targets within this module. **Table 4** highlights the top 10% of targets scored for each disease, revealing 12 common targets shared across these categories (see **Table 5 and Table S5**). These targets are involved in 159 pathways, reduced from an initial 227, as detailed in **Table S6**.

Table 3. List of disease conditions for the reported potential therapeutic effects of DBT.

Relevant diseasea	Disease category
Ulcerative colitis, chronic non-healing ulcers, Rheumatoid arthritis	Immune system disease
Menstrual anemia, myelosuppression, chemotherapy-induced bone marrow suppression, blood deficiency, anemia	Hematologic disease
Non-small-cell lung cancer, breast cancer, lung cancer, metastatic colon cancer	Cancer
Atherosclerosis, Myocardial infarction, coronary heart disease (CHD)	Cardiovascular disease
Diabetic nephropathy (DN)	Metabolic disease; endocrine disease; Urinary system disease
Parkinson's disease, vascular dementia	Neurodegenerative disease
Age-related macular degeneration	Nervous system disease
Non-proliferative diabetic retinopathy	Endocrine and metabolic disease; Nervous system disease
Idiopathic pulmonary fibrosis	Respiratory system disease
Premature ovarian failure	Reproductive system disease

[a]The grouping by their primary disease categories based on KEGG disease database system-level classification is obtained from https://www.genome.jp/kegg/disease/ for each disease.

Table 4: Gene targets from module 3 with contribution scores rank in the top 10% for each disease category.

Disease Categorya	Target Genes
Nervous system disease	GSK3B, AKT1, SRC, BAX, CCND1, MAPK3, MAPK1, MTOR, EGFR, RAF1, PIK3R1, PIK3CD, PIK3CA, PLCG1, PRKCB, PRKCA, TP53
Immune system disease	IGF1, AKT1, SRC, BAX, CCND1, MAPK3, MAPK1, MTOR, EGFR, RAF1, PIK3R1, PIK3CD, PIK3CA, PLCG1, PRKCB, PRKCA, TP53
Hematologic disease	GSK3B, AKT1, SRC, BAX, CCND1, MAPK3, MAPK1, MTOR, CDKN1A, EGFR, RAF1, PIK3R1, PIK3CD, PIK3CA, PRKCB, PRKCA, TP53
Neurodegenerative disease	IGF1, GSK3B, AKT1, SRC, BAX, MAPK3, MAPK1, MTOR, EGFR, RAF1, PIK3R1, PIK3CD, PIK3CA, PLCG1, PRKCB, PRKCA, TP53
Cardiovascular disease	IGF1, GSK3B, AKT1, SRC, CCND1, MAPK3, MAPK1, MTOR, EGFR, RAF1, PIK3R1, PIK3CD, PIK3CA, PLCG1, PRKCB, PRKCA, TP53
Urinary system disease	IGF1, GSK3B, AKT1, SRC, CCND1, MAPK3, MAPK1, EGFR, RAF1, PTK2, PIK3R1, PIK3CD, PIK3CA, PLCG1, PRKCB, PRKCA, TP53
Cancer	GSK3B, AKT1, SRC, BAX, CCND1, MAPK3, MAPK1, MTOR, EGFR, RAF1, PIK3R1, PIK3CD, PIK3CA, PLCG1, PRKCB, PRKCA, TP53

[a] Each row lists a system-level disease classification with the corresponding high-scoring genes. The associated protein names and UniProt links for each gene are provided in Table S5.

AKT1 and PIK3R1 (with PIK3CA and PIK3CD) are the core components of PI3K/Akt signaling pathway: this pathway governs cell survival, proliferation and metabolism, and is often being hyperactivated in cancers [21]. Besides, PI3K/Akt activation protects the heart by limiting infarct

© 2025 by the author(s). Distributed under a Creative Commons CC BY license.

Preprints.org (www.preprints.org) | NOT PEER-REVIEWED | Posted: 5 September 2025 doi:10.20944/preprints202509.0511.v1

damage and promoting recovery after ischemia [22]. **Table 5** and **Figure 5** show the nine functional compounds in the herbal decoction being linked to the top-scoring proteins. Quercetin stands out as the central compound, interacting with nearly all targets, except PIK3CD. Calycosin and formononetin follow, engaging with seven and four targets, respectively. Both calycosin and formononetin are known for their hematopoietic and blood-enriching effects [9], which contribute to these processes by stimulating EPO, a key factor in red blood cell production [23]. Additionally, formononetin exhibits anti-inflammatory and anti-atherogenic effects by lowering the expressions of adhesion molecules, e.g., VCAM-1 and ICAM-1, in cultured endothelial cells [24].

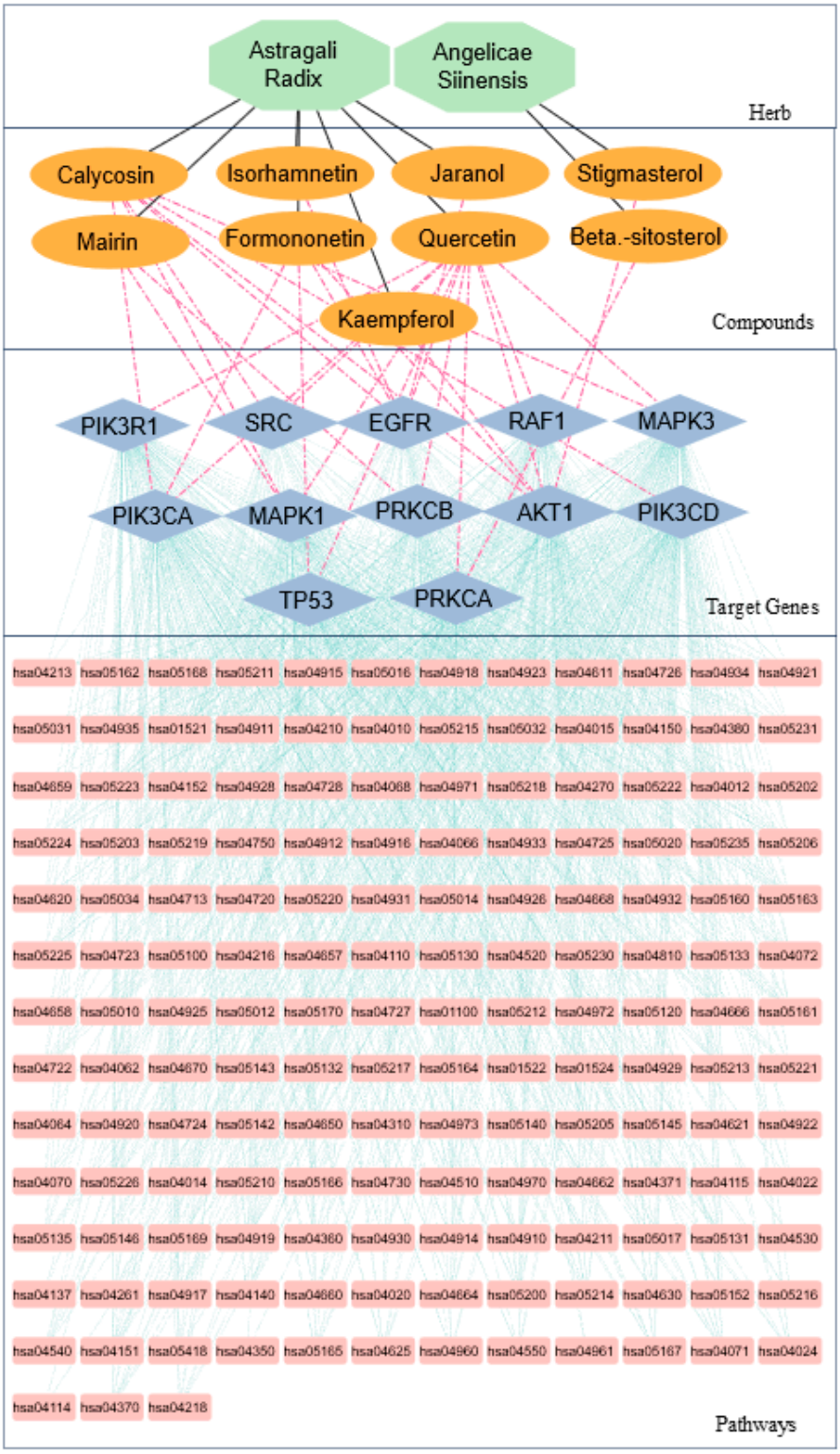

© 2025 by the author(s). Distributed under a Creative Commons CC BY license.

Preprints.org (www.preprints.org) | NOT PEER-REVIEWED | Posted: 5 September 2025 doi:10.20944/preprints202509.0511.v1

Figure 5. Integration of Herbs–Compound–Target–Pathway network filtered on Module 3 top contributors. These genes mapped 153 of the 227 enriched KEGG pathways, and their original DBT compounds and the source herbs were then assembled into the network. The resulting network links these targets to their corresponding DBT compounds and source herbs, highlighting key bioactive interactions. Nodes are encoded by both shape and color—octagons represent herbs, ovals compounds, diamonds genes, and rectangles pathways—and edges represent herb–compound (solid black), compound–target (pink dashed), and target–pathway (thin green dashed) relationships. This overview highlights the principal bioactive compounds and signaling pathways through which Module 3 may mediate the therapeutic effects of DBT in the selected disease categories.

Table 5. Core module 3 target proteins and their relevant bioactive compounds from Astragali Radix and Angelicae Sinensis Radix.

Gene Symbol[a]	Uniport ID	Relevant Compound (source herb) [b]
AKT1	P31749	Formononetin (AR), Stigmasterol (AS), Kaempferol (AR), Quercetin (AR), Calycosin (AR)
EGFR	P00533	Formononetin (AR), Quercetin (AR), Jaranol (AR), Isorhamnetin (AR), Calycosin (AR)
MAPK1	P28482	Calycosin (AR), Mairin (AR), Quercetin (AR)
MAPK3	P27361	Calycosin (AR), Quercetin (AR)
PIK3CA		Calycosin (AR), Formononetin (AR), Quercetin (AR)
PIK3CD	P42336	Calycosin (AR)
PIK3R1	P27986	Quercetin (AR)
PRKCA	P17252	Beta-sitosterol (ASR), Quercetin (AR)
PRKCB	P05771	Mairin (AR), Quercetin (AR)
RAF1	P04049	Quercetin (AR)
SRC	P12931	Calycosin (AR), Quercetin (AR)
TP53	P04637	Formononetin (AR), Quercetin (AR)

[a] The listing each gene symbol with Primary accession (UniProt ID) and the associated herbal ingredients. [b] AR: Astragali Radix and ASR: Angelicae Sinensis Radix.

DBT and its active flavonoids, e.g., quercetin, kaempferol, could treat premature ovarian failure (induced by cyclophosphamide (CTX)) in rats, by regulating the balance of estrogen receptors and androgen receptors through the interacting TP53 and AKT pathways, which jointly control ovarian cell apoptosis and hormone receptor signaling [25]. In DSS-induced ulcerative colitis mouse model, DBT alleviated colon inflammation and mucosal damage by inhibiting the PI3K/Akt signaling pathway: AKT1, SRC, EGFR were among core gene highlighted by network pharmacology [14]. In a mouse model of acute renal injury, the treatment of DBT demonstrated a protective effect on renal function, evidenced by significant reductions in serum BUN and creatinine levels, as well as alleviation of renal edema. Mechanistically, this effect was attributed to the interaction of multiple active constituents with key targets, including EGFR, AKT1, PIK3CA, MAPK1 and SRC as identified through network pharmacology and further supported by molecular docking analyses. 3,9-di-O-methylnissolin, (6aR,11aR)-9,10-dimethoxy-6a, 11a-dihydro-6H-benzofurano[3,2-c] chromen-3-ol, (3R)-3-(2-hydroxy-3,4-dimethoxyphenyl) chroman-7-ol, jaranol, kaempferol, and 7-O-methylisomucronulatol were top six core ingredients [26]. Besides, DBT enhanced the adhesion and migration of bone marrow cells by activating the PI3K/Akt and focal adhesion signaling pathways, suggesting its potential to promote hematopoietic activity and support blood regeneration [27].

DBT may exert nephroprotective effects in diabetic nephropathy by inhibiting the AGEs/RAGE signaling pathway and its downstream PI3K/AKT cascade (as listed in **Table S5**) and thereby reducing oxidative stress, inflammation, and kidney injury in diabetic mice. Active compounds, such as calycosin-7-O-β-D-glucoside, calycosin, formononetin, chlorogenic acid, ferulic acid, caffeic acid, and Z-ligustilide, identified through anti-glycation and MTT assays, are the key bioactive constituents of DBT contributing to its therapeutic effect against diabetic nephropathy [28]. DBT

© 2025 by the author(s). Distributed under a Creative Commons CC BY license.

Preprints.org (www.preprints.org) | NOT PEER-REVIEWED | Posted: 5 September 2025 doi:10.20944/preprints202509.0511.v1

alleviates diabetic nephropathy by modulating lipid metabolism (particularly sphingolipid and glycerophospholipid pathways (**Table S5**) and regulating inflammatory and insulin signaling pathways through a combination of lipidomics, transcriptomics, and network pharmacology analyses [29].

In network pharmacology analyses, quercetin and kaempferol, the principal bioactive compounds in DBT, were identified as core agents, with TP53, AKT1, and inflammatory mediators, such as TNF and IL-6, emerging as key targets involved in plaque stability regulation. Subsequent cell-based studies demonstrated that both quercetin and kaempferol significantly inhibited foam cell formation, via downregulation of these targets, thereby contributing to enhanced stability of atherosclerotic plaques [16]. In a rat model of myocardial infarction, DBT exhibited notable cardioprotective effects, including reduced infarct size and decreased myocardial infarction-induced apoptosis in cardiomyocytes. Network pharmacology and molecular docking analyses identified quercetin, kaempferol, isoflavanones, isorhamnetin, hederagenin, and formononetin as core bioactive compounds. These compounds showed high binding affinity to key target proteins, i.e., AKT1, ERK2, and CASPASE-9, which are implicated in the PI3K/AKT signaling pathway, suggesting a mechanistic basis for DBT's action. However, further experimental validation is needed to confirm these interactions [17]. In another work, DBT enhanced angiogenesis in myocardial infarction rats by modulating the VEGF signaling pathway (also listed in **Table S5**), increasing VEGF and VEGFR1/2 expression, decreasing VEGFR1/2, and improving cardiac function while reducing fibrosis [30]. The herb-pair Astragali Radix and Angelicae Sinensis Radix suppresses breast cancer growth by upregulating PIK3R1 (seen as hub gene in network analysis), with quercetin and suchilactone synergistically enhancing immune activation and inhibiting tumor cell viability, highlighting their potential as a novel anti-cancer therapy [31].

There are several limitations to this research work that should be acknowledged. First, the target mining for compounds was conducted using public databases, which means that some of the targets identified are predicted and require further validation to confirm their biological relevance. Second, the concentration and ratio of the herbs used in clinical settings may influence therapeutic outcomes, but this factor is often not considered in network pharmacology studies, potentially impacting the applicability of the findings. Lastly, certain compounds known for their therapeutic effects, such as ferulic acid, ligustilide, and astragalosides, were excluded from the initial target list because they did not meet the ADME filtering criteria, which may limit the comprehensiveness of the analysis.

3. Materials and Methods

3.1. Compound Acquisition

The Traditional Chinese Medicine Systems Pharmacology Database and Analysis Platform (TCMSP, http://tcmspw.com/tcmsp.php) was interrogated to identify bioactive constituents of two herbal medicines: Astragali Radix using the search term "Huangqi" and Angelicae Sinensis Radix using the term "Danggui." Candidate compounds were filtered based on pharmacokinetic parameters, including an oral bioavailability (OB) threshold >30% and drug-likeness (DL) criteria >0.18, consistent with established ADME screening protocols [14,16,25].

3.2. Protein Targets Mining

Initial target profiles for both herbs were extracted from TCMSP, followed by Uniprot database cross-referencing to obtain standardized gene nomenclature and primary accession IDs limited to *Homo sapiens* entries with Swiss-Prot reviewed status. Target identification was expanded through interrogation of two additional resources: ETCM v2.0 [32] (http://www.tcmip.cn/ETCM2/front/#/) and Herb v2.0 [33] (http://47.92.70.12/), incorporating both experimentally validated and computationally predicted targets. Complementary target prediction was performed via Swiss Target Prediction using canonical SMILES representations of compounds, retaining only high-confidence predictions (probability score >0.8).

© 2025 by the author(s). Distributed under a Creative Commons CC BY license.

Preprints.org (www.preprints.org) | NOT PEER-REVIEWED | Posted: 5 September 2025 doi:10.20944/preprints202509.0511.v1

3.3. Functional Enrichment Analysis and Disease Category Mapping

Protein targets were analyzed using the STRING database (v12.0) (https://version-12-0.string-db.org/api/tsv/enrichment) and a false discovery rate (FDR) threshold <0.05 to conduct Gene Ontology (GO) enrichment analysis (biological process, cellular component, molecular function) and Kyoto Encyclopedia of Genes and Genomes (KEGG) pathway enrichment. Pathway classifications were extracted from KEGG pathway metadata ("Class" field in https://www.kegg.jp/kegg/pathway.html). Disease associations were established by mapping constituent genes of each pathway to KEGG disease entries via the KEGG REST API (https://rest.kegg.jp/link/hsa/path: {PathwayIdentifier}; https://rest.kegg.jp/link/disease/hsa: {gene}). Disease categories were derived from hierarchical descriptors in KEGG disease records (https://www.kegg.jp/entry/{H-coded_disease_ identifier}).

3.4. Network Construction and Module Identification

A target-pathway-target network was generated by establishing edges between gene pairs exhibiting shared participation in ≥1 KEGG pathway. The cardinality of co-enriched pathways served as edge weight determinants. Network visualization and topological analysis were implemented in Cytoscape 3.10.3, with gene pairs imported as source-target node pairs and edge weights assigned via adjacency matrices. Community/Module detection was executed via the Louvain algorithm with cluster resolution = 1.0 [19,20] (with weight variable to be edge weights (number of shared pathways between each pairs) in CyCommunity Detection App [34] in Cytoscape.

3.5. Contribution Score Calculation

A therapeutic association metric (contribution score, CS) was employed to quantify the module-disease relationships by incorporating target-pathway and pathway-disease relationships, derived from methodologies established by Zuo et al. [19] and algorithmically refined by Chen et al. [20]. This algorithm calculates the contribution score of each target gene for each disease based on its contribution to each pathway relevant to that specific disease category, normalized by the number of proteins participating in that pathway and the number of pathways associated with each disease category within the gathered dataset (consult primary references for computational formalism). Contribution scores were calculated for individual targets to prioritize their roles, with the top 10% of targets based on these scores systematically selected as candidate therapeutic targets for subsequent studies investigating the mechanism of action of DBT herbal decoction.

4. Conclusion

This study presents a network pharmacology approach to understand how the Chinese herbal mixture DBT works. By integrating compound, protein target, and enriching pathway information, we constructed a TPT network and identified key modules being linked to DBT's therapeutic effects. The different modules represent the multi-faceted or multi-therapeutic nature of the herbal mixture. Among these, module 3 stood out for its strong association with the well-known actions of DBT, featuring several protein targets, many of which have been previously reported to play important roles in DBT's pharmacological activity. Combined with a contribution scoring algorithm, the TPT network shows strong potential for analyzing traditional medicines, especially those with established clinical relevance. This network-based strategy provides a more focused and efficient way to uncover potential therapeutic targets across different disease categories.

Supplementary Materials: The following supporting information can be downloaded at the website of this paper posted on Preprints.org.

© 2025 by the author(s). Distributed under a Creative Commons CC BY license.

Preprints.org (www.preprints.org) | NOT PEER-REVIEWED | Posted: 5 September 2025 doi:10.20944/preprints202509.0511.v1

References

1. Kwan, K. K. L.; Huang, Y.; Leung, K. W.; Dong, T. T. X.; Tsim, K. W. K. Danggui Buxue Tang, a Chinese herbal decoction containing Astragali Radix and Angelicae Sinensis Radix, modulates mitochondrial bioenergetics in cultured cardiomyoblasts. Front Pharmacol. **2019**, 10, 614. doi: 10.3389/fphar.2019.00614.
2. Lin, H. Q.; Gong, A. G. W.; Wang, H. Y.; Duan, R.; Dong, T. T. X.; Zhao, K. J.; Tsim, K. W. K. Danggui Buxue Tang (Astragali Radix and Angelicae Sinensis Radix) for menopausal symptoms: A review. J Ethnopharmacol. **2017**, 199, 205–10. doi: 10.1016/j.jep.2017.01.044.
3. Gong, A. G.; Zhang, L. M.; Lam, C. T.; Xu, M. L.; Wang, H. Y.; Lin, H.; Dong, T. T.; Tsim, K. W. Polysaccharide of Danggui Buxue Tang, an ancient Chinese herbal decoction, induces expression of pro-inflammatory cytokines possibly via activation of NFKB signaling in cultured raw 264.7 cells. Phytother Res. **2017**, 31(2), 274–83. doi: 10.1002/ptr.5745.
4. Liu, D.; Mu, Y.; Gao, F.; Zhang, Y.; Shen, Z.; Zhao, Z.; Zhang, P.; Lv, T.; Wang, Y.; Liu, Y. Multi-tissue metabolomics and network pharmacology study on the intervention of Danggui Buxue Decoction in mice with gemcitabine induced myelosuppression. J Ethnopharmacol. **2025**, 343, 119498. doi: 10.1016/j.jep.2025.119498.
5. Guo, R.; Guo, S.; Gao, X.; Wang, H.; Hu, W.; Duan, R.; Dong, T. T. X.; Tsim, K. W. K. Fermentation of Danggui Buxue Tang, an ancient Chinese herbal mixture, together with Lactobacillus plantarum enhances the anti-diabetic functions of herbal product. Chin Med. **2020**, 15(1), 98. doi: 10.1186/s13020-020-00379-x.
6. Huang, Y.; Kwan, K. K. L.; Leung, K. W.; Wang, H.; Kong, X. P.; Dong, T. T. X.; Tsim, K. W. K. The extracts and major compounds derived from Astragali Radix alter mitochondrial bioenergetics in cultured cardiomyocytes: comparison of various polar solvents and compounds. Int J Mol Sci. **2018**, 19(6), 1574. doi: 10.3390/ijms19061574.
7. Gong, A. G. W.; Huang, V. Y.; Wang, H. Y.; Lin, H. Q.; Dong, T. T. X.; Tsim, K. W. K. Ferulic acid orchestrates anti-oxidative properties of Danggui Buxue Tang, an ancient herbal decoction: elucidation by chemical knock-out approach. PLOS ONE. **2016**, 11(11), e0165486. doi: 10.1371/journal.pone.0165486.
8. Li, C.; Zhu, F.; Wang, S.; Wang, J.; Wu, B. Danggui Buxue Decoction ameliorates inflammatory bowel disease by improving inflammation and rebuilding intestinal mucosal barrier. Evid Based Complement Alternat Med. **2021**, 2021, 1–12. doi: 10.1155/2021/8853141.
9. Shi, X. Q.; Yue, S. J.; Tang, Y. P.; Chen, Y. Y.; Zhou, G. S.; Zhang, J.; Zhu, Z. H.; Liu, P.; Duan, J. A. A network pharmacology approach to investigate the blood enriching mechanism of Danggui Buxue Decoction. J Ethnopharmacol. **2019**, 235, 227–42. doi: 10.1016/j.jep.2019.01.027.
10. Hua, Y. L.; Ma, Q.; Yuan, Z. W.; Zhang, X. S.; Yao, W. L.; Ji, P.; Hu, J. J.; Wei, Y. M. A novel approach based on metabolomics coupled with network pharmacology to explain the effect mechanisms of Danggui Buxue Tang in anaemia. Chin J Nat Med. **2019**, 17(4), 275–90. doi: 10.1016/S1875-5364(19)30031-7.
11. Liu, Y.; Ju, Y.; Qin, X. Studies on the compatibility mechanism and material basis of Danggui Buxue Decoction against anemia mice using metabonomics and network pharmacology. J Pharm Pharmacol. **2021**, 73(6), 767–77. doi: 10.1093/jpp/rgab016.
12. Yu, B.; Lv, G.; Li, Z.; Li, Y.; Xu, H. Utilizing bioinformatics technology to explore the potential mechanism of Danggui Buxue Decoction against NSCLC. Dis Markers. **2022**, 2022, 5296830. doi: 10.1155/2022/5296830.
13. Zhu, D.; Li, S.; Xu, L.; Ren, X.; Wang, S.; Chen, J.; Zhao, E.; Zheng, Z. Investigation of the molecular mechanism of Danggui Buxue Tang in treating lung cancer using network pharmacology and molecular docking techniques. Nat Prod Res. **2025**, 39(11), 3312–5. doi: 10.1080/14786419.2024.2305660.
14. Liu, W. J.; Ma, S. B.; Li, J. X.; Fan, B. S.; Du, Y.; Xu, Z. H.; Li, X. Q.; Cao, W.; Tang, Y. P. Explore the key targets and mechanism of Danggui Buxue Decoction against ulcerative colitis: Network pharmacology and experimental validation. J Ethnopharmacol. **2025**, 344, 119580. doi: 10.1016/j.jep.2025.119580.
15. Xu, H.; Zhang, T.; He, L.; Yuan, M.; Yuan, X.; Wang, S. Exploring the mechanism of Danggui Buxue Decoction in regulating atherosclerotic disease network based on integrated pharmacological methods. Biosci Rep. **2021**, 41(10), BSR20211429. doi: 10.1042/BSR20211429.
16. Zheng, G.; Cao, X.; Jing, Y.; Wang, L.; Yan, R.; Ji, Y.; Zhang, Y.; Li, H.; Wang, Y.; Shi, Y.; Yu, Y.; Xiong, Q. An integrative approach for mechanistic insights into the atherosclerotic plaque-stabilizing properties of Danggui Buxue Decoction. J Ethnopharmacol. **2025**, 343, 119450. doi: 10.1016/j.jep.2025.119450.

© 2025 by the author(s). Distributed under a Creative Commons CC BY license.

Preprints.org (www.preprints.org) | NOT PEER-REVIEWED | Posted: 5 September 2025 doi:10.20944/preprints202509.0511.v1

17. Shen, C.; Chen, Q.; Chen, S.; Lin, Y. Mechanism of Danggui Buxue Decoction in the treatment of myocardial infarction based on network pharmacology and experimental identification. Heliyon. **2024**, 10(8), e29360. doi: 10.1016/j.heliyon.2024.e29360.
18. Fan, Q.; Liu, X.; Zhang, Y.; Kang, W.; Si, S.; Zhang, H. Integration of metabolomics and network pharmacology technology to explain the effect mechanisms of Danggui Buxue Decoction in vascular dementia. Biomed Chromatogr. **2024**, 38(4), e5822. doi: 10.1002/bmc.5822.
19. Zuo, H.; Zhang, Q.; Su, S.; Chen, Q.; Yang, F.; Hu, Y. A network pharmacology-based approach to analyse potential targets of traditional herbal formulas: An example of Yu Ping Feng Decoction. Sci Rep. **2018**, 8(1), 11418. doi: 10.1038/s41598-018-29764-1.
20. Chen, J.; Teng, D.; Wu, Z.; Li, W.; Feng, Y.; Tang, Y.; Liu, G. Insights into the molecular mechanisms of Liuwei Dihuang Decoction via network pharmacology. Chem Res Toxicol. **2021**, 34(1), 91–102. doi: 10.1021/acs.chemrestox.0c00359.
21. He, Y.; Sun, M. M.; Zhang, G. G.; Yang, J.; Chen, K. S.; Xu, W. W.; Li, B. Targeting PI3K/AKT signal transduction for cancer therapy. Signal Transduct Target Ther. **2021**, 6(1), 425. doi: 10.1038/s41392-021-00828-5.
22. Deng, R. ming; Zhou, J. The role of PI3K/AKT signaling pathway in myocardial ischemia-reperfusion injury. Int Immunopharmacol. **2023**, 123, 110714. doi: 10.1016/j.intimp.2023.110714.
23. Yu, H.; Zhang, W. L.; Ding, X.; Zheng, K. Y. Z.; Ho, C. M.; Tsim, K. W. K.; Lee, Y. K. Optimizing combinations of flavonoids deriving from Astragali Radix in activating the regulatory element of erythropoietin by a feedback system control scheme. Evid Based Complement Alternat Med. **2013**, 2013, 1–10. doi: 10.1155/2013/541436.
24. De Andrade, C. M.; De Sá, M. F. S.; Toloi, M. R. T. Effects of phytoestrogens derived from soy bean on expression of adhesion molecules on HUVEC. Climacteric. **2012**, 15(2), 186–94. doi: 10.3109/13697137.2011.582970.
25. Liu, H.; Yang, H.; Qin, Z.; Chen, Y.; Yu, H.; Li, W.; Zhu, X.; Cai, J.; Chen, J.; Zhang, M. Exploration of the Danggui Buxue Decoction mechanism regulating the balance of ESR and AR in the TP53-AKT signaling pathway in the prevention and treatment of POF. Evid Based Complement Alternat Med. **2021**, 2021, 1–16. doi: 10.1155/2021/4862164.
26. Lou, X.; Ma, Y.; Deng, J.; Lv, Y.; Li, R.; Shang, M.; Zhang, Q.; Zhang, X.; Hou, T. Exploring the mechanism of Danggui Buxue Decoction against acute renal insufficiency using network pharmacology and molecular docking. Mol Cell Biomech. **2024**, 21(3), 388. doi: 10.62617/mcb388.
27. Bo, H.; He, J.; Wang, X.; Du, R.; Bei, H.; Chen, J.; Wang, J.; Wu, F.; Zhang, W.; Chen, Q. Danggui Buxue Tang promotes the adhesion and migration of bone marrow stromal cells via the focal adhesion pathway in vitro. J Ethnopharmacol. **2019**, 231, 90–7. doi: 10.1016/j.jep.2018.11.018.
28. Zhang, Z. T.; Qi, Y.; Chen, P.; Chen, L.; Jiang, Y.; Fan, Z.; Guan, H.; Bai, L.; Liu, J.; Zhao, D.; Yan, G. Dang-Gui-Bu-Xue decoction against diabetic nephropathy via modulating the carbonyl compounds metabolic profile and AGEs/RAGE pathway. Phytomedicine. **2024**, 135, 156104. doi: 10.1016/j.phymed.2024.156104.
29. Sun, L.; Yang, Z.; Zhao, W.; Chen, Q.; Bai, H.; Wang, S.; Yang, L.; Bi, C.; Shi, Y.; Liu, Y. Integrated lipidomics, transcriptomics and network pharmacology analysis to reveal the mechanisms of Danggui Buxue Decoction in the treatment of diabetic nephropathy in type 2 diabetes mellitus. J Ethnopharmacol. **2022**, 283, 114699. doi: 10.1016/j.jep.2021.114699.
30. Hu, G.; Yang, P.; Zeng, Y.; Zhang, S.; Song, J. Danggui Buxue Decoction promotes angiogenesis by up-regulation of VEGFR1/2 expressions and down-regulation of sVEGFR1/2 expression in myocardial infarction rat. J Chin Med Assoc. **2018**, 81(1), 37–46. doi: 10.1016/j.jcma.2017.06.015.
31. Liu, H.; Lian, L.; Hou, L.; Liu, C.; Ren, J.; Qiao, Y.; Wen, S.; Li, Q. Herb pair of Huangqi-Danggui exerts anti-tumor immunity to breast cancer by upregulating PIK3R1. Anim Models Exp Med. **2024**, 7(3), 234–58. doi: 10.1002/ame2.12434.
32. Zhang, Y.; Li, X.; Shi, Y.; Chen, T.; Xu, Z.; Wang, P.; Yu, M.; Chen, W.; Li, B.; Jing, Z.; Jiang, H.; Fu, L.; Gao, W.; Jiang, Y.; Du, X.; Gong, Z.; Zhu, W.; Yang, H.; Xu, H. ETCM v2.0: An update with comprehensive resource and rich annotations for traditional Chinese medicine. Acta Pharm Sin B. **2023**, 13(6), 2559–71. doi: 10.1016/j.apsb.2023.03.012.

© 2025 by the author(s). Distributed under a Creative Commons CC BY license.

Preprints.org (www.preprints.org) | NOT PEER-REVIEWED | Posted: 5 September 2025 doi:10.20944/preprints202509.0511.v1

33. Gao, K.; Liu, L.; Lei, S.; Li, Z.; Huo, P.; Wang, Z.; Dong, L.; Deng, W.; Bu, D.; Zeng, X.; Li, C.; Zhao, Y.; Zhang, W.; Wang, W.; Wu, Y. HERB 2.0: an updated database integrating clinical and experimental evidence for traditional Chinese medicine. Nucleic Acids Res. **2025**, 53(D1), D1404–14. doi: 10.1093/nar/gkae1037.
34. Singhal, A.; Cao, S.; Churas, C.; Pratt, D.; Fortunato, S.; Zheng, F.; Ideker, T. Multiscale community detection in Cytoscape. PLOS Comput Biol. **2020**, 16(10), e1008239. doi: 10.1371/journal.pcbi.1008239.

Disclaimer/Publisher's Note: The statements, opinions and data contained in all publications are solely those of the individual author(s) and contributor(s) and not of MDPI and/or the editor(s). MDPI and/or the editor(s) disclaim responsibility for any injury to people or property resulting from any ideas, methods, instructions or products referred to in the content.

© 2025 by the author(s). Distributed under a Creative Commons CC BY license.